

# An animat's cell doctrine

Lisa Schramm<sup>1</sup> and Bernhard Sendhoff<sup>2</sup>

<sup>1</sup>Technische Universität Darmstadt, Karolinenplatz 5, 64289 Darmstadt, Germany

<sup>2</sup>Honda Research Institute Europe, Carl-Legien-Str. 30, 63073 Offenbach, Germany  
lschramm@rtr.tu-darmstadt.de

## Abstract

We present a developmental model to simulate swimming digital organisms following an animat's cell doctrine. Morphology and control are encoded in one genome concurrently using artificial cells as the basic building blocks for both. Each individual starts with one cell in the middle of a computational environment, and its development is controlled by a gene regulatory network. The cells can differentiate into central pattern generators that control the movements of the resulting individual. After the developmental process, the individual is placed into a physics simulation environment and the distance it swims in a defined time is evaluated. Contrary to most existing models, one genome for both, morphology and control is used and the CPGs representing the dynamic control contribute to the morphology of the organism.

## Introduction

Following the work of Matthias Jakob Schleiden on plant tissues, Theodor Schwann postulated in 1839 that the tissue of all living organisms is made up of individual cells. At first this excluded the nervous system, which was later rectified by the seminal neuro-anatomical work of Ramón y Cajal and others. This principal concept is known as the cell or the neuron doctrine of biology.

In biology, the cell doctrine (including the nervous system) is an integral part of the evolution, development and operation of all living organisms. The cell as the carrier of the hereditary information is not just the basic functional unit of organisms, it is also the basic unit for the evolutionary process. Turning this argument around, we can hypothesize that the direction of the evolutionary process and its diverse results are a consequence of the cell doctrine. More strongly, evolution would have not been successful<sup>1</sup> without the cell as its basic unit. We also note that most of the evolutionary history has been devoted to single cell organisms rather than to multicellular ones.

<sup>1</sup>What does it mean, evolution being successful? To circumvent a philosophical discussion, we will resort to an artificial life perspective, equating success with progress in the criterion chosen for the process.

In artificial life, biological paradigms are frequently sought to facilitate the development of digital organisms or animats. The purpose of this paper is to outline a model that allows the simulation of digital organisms based on basic cell-like units, thus paving the way to an animat's cell doctrine including the nervous system or in more abstract terms the control system of the animat.

Since the seminal work of Karl Sims (Sims, 1994) the co-evolution of the morphology (=body) and the control systems (=brain) of digital organisms has received continuous attention. In Sim's work a developmental model using a directed graph has been used for both neural controller and body plan. The role of the morphology to reach a certain functionality has also been discussed in robotics. The passive walker (McGeer, 1990) demonstrated convincingly how the specific mechanical configuration alone can lead to a walking behavior that closely resembles the one we observe in humans without complex control algorithms. However, not least due to the mechanical difficulties the body is mainly unchanged in most evolutionary or developmental robotics approaches. Evolving the developmental steps of a controller in a static morphology has no justification and its limitations have been recognized, see e.g. (Pfeifer et al., 2007). Although some advances have been made using mechanical cell blocks to enable a changing morphology, the mechanical restrictions are still fundamental (Murata and Kurokawa, 2007; Meng et al., 2011).

In the digital world, we face much fewer restrictions and it is possible to simulate completely cell based animats, see e.g. (Schramm et al., 2009). Several computer models for brain-body co-evolution have been proposed in the literature, see e.g. (Hornby and Pollack, 2001; Miconi and Channon, 2006; Spector et al., 2007). However, models have either been detailed with regard to neural development (Kitano, 1995) or with the development of the morphology (Andersen et al., 2009; Eggenberger Hotz et al., 2003). Using a more abstract representation for the body morphology, Jones et al. (2011, 2008) analyzed the effects of the body plan on neural organization using energy constraints. Bongard and Paul (2000) studied the correlation between morphological

symmetry and locomotive efficiency using a direct encoding. The advantage of being able to evolve a bilaterally symmetric body plan or neural controller has been reported independently in (Mazzapioda et al., 2009; Oros et al., 2009). Bongard (2003) uses a gene regulatory model to develop locomoting animats or animats that should grow to touch an object.

A number of computational models have been developed to model biological gene regulatory networks (see e.g. the review of de Jong (2002)). Artificial embryogeny simulates biological cellular growth and pattern formation starting with one single cell (Andersen et al., 2009; Eggenberger Hotz et al., 2003; Harding and Banzhaf, 2008; Joachimczak and Wröbel, 2009; Doursat, 2009; Kowaliw et al., 2004). Steiner et al. (2008) evolved the structure and the parameters of a gene regulatory network for growing 3D cellular structures that are mechanically stable and lightweight. The model was refined in (Steiner et al., 2009) using cell polarization to represent more complex inner structures. Stanley and Miikkulainen (2003) develop a taxonomy for artificial embryogeny based on cell fate, targeting, heterochrony, canalization, and complexification.

In this contribution, we implement an animat’s cell doctrine by representing the whole body or morphology of the digital organism by cells some of which perform the control of the animat’s behavior. Therefore, the nervous system is an integral part of the morphology and the neurons are basic cells that differentiate during embryogeny assuming their specific neural functionality. Therefore, the system evolves the shape and the control of animats concurrently. Furthermore, the representations of shape and control are not separated, instead morphology and control are phenotypic characteristics of the artificial organisms that are the result of a common gene regulatory network that organizes the cellular growth of the animat. Indeed the separation between morphology and control becomes arbitrary even on the phenotypic level, because the cells that control the behavior also contribute to the morphology of the animat. This straightforwardly results from using artificial cells as the basic structural as well as functional components of our animat.

For the simulation of the cellular neural control we use central pattern generators (CPGs) which represent a higher level of abstraction compared to the spiking neural system employed in (Jin et al., 2008). CPGs facilitate the evolution of an oscillating movement, which makes it easier for the evolutionary process to develop the swimming behavior.

In the next section, we introduce CPGs in general and the specific CPG model used in this paper in greater detail. The following section is devoted to a description of our model of gene regulatory networks (GRNs) and how it is used to represent cellular growth. Thereafter, the physics simulation and the experiments are described followed by a discussion of the results. In the last section, the main findings of the paper are summarized and an outlook into future experiments

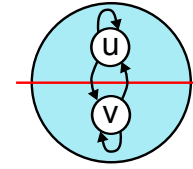


Figure 1: The model of a central pattern generator contains two neurons that interact with each other.

Table 1: Properties of the CPG Model

$k$	$\omega$	$\rho$	$\lambda$	$\sigma$
0.01	0.3	1	1	1

is presented.

## Central Pattern Generators (CPGs)

Many animals use coupled rhythmic muscle activations for movements. This movement is not controlled by the brain, but by coupled oscillators, the central pattern generators (CPG). It can be shown, that the pattern occurs also after the spinal cord has been separated from the brain (Murray, 2008).

Several models of CPGs exist, e.g. (Murray, 2008; Ijspeert and Kodjabachian, 1999; Verdaasdonk et al., 2006; Chung and Slotine, 2010; Beer, 2009), in general the CPG consists of two neurons which interact with each other, see Figure 1. The difficulty with most models is the stability of the output of many CPGs depending on their connections. The output of the CPGs should ideally be sinusoidal with phase shifts between the output signals of the different CPGs depending on their synapse connections and weights. Each CPG oscillates, they synchronize with other CPGs using their connections, so no global clock is used.

Chung and Slotine (2010) use coupled Hopf-Kuramoto oscillators and show their ability to synchronize almost globally. This model is used for the experiments presented in the following because of its good ability to synchronize. Therefore,  $\mathbf{x}_i(t) = (u_i(t), v_i(t))^T$  and the following equations are used:

$$\dot{\mathbf{x}}_i = \mathbf{f}(\mathbf{x}_i; \rho_i) - k \sum_{j \in \mathcal{N}_i}^{m_i} \left( \mathbf{x}_i - \frac{\rho_i}{\rho_j} \mathbf{R}(\phi_{ij}) \mathbf{x}_j \right) \quad (1)$$

and

$$\mathbf{f}(\mathbf{x}; \rho) = \begin{pmatrix} -\lambda/\rho^2 (u^2 + v^2 - \rho^2\sigma) u - \omega(t)v \\ \omega(t)u - \lambda/\rho^2 (u^2 + v^2 - \rho^2\sigma) v \end{pmatrix}. \quad (2)$$

The properties of the model for the simulations in this paper are described in Table 1.

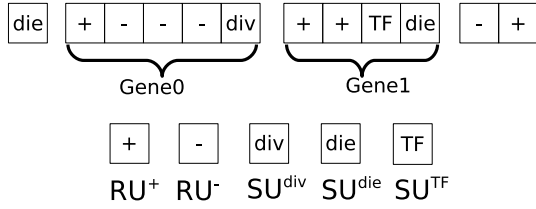


Figure 2: An example chromosome for the development. The first gene (gene 0) starts at the first RU of the genome. Each SU-RU changeover defines a boundary between two genes.

## A Computational Model for the Development of Morphology and Control

The morphological development simulated in this work is under the control of a gene regulatory network (GRN) and physical cellular interactions. The morphological development starts with a single cell put in the center of a two-dimensional computational area of size  $100 \times 80$ . Each cell can die or divide. The cells are not fixed on a grid and underlie physical interactions, i.e. overlapping cells push each other away and cells that do not overlap attract each other with decreasing forces with larger distances.

The GRN is defined by a set of genes, each consisting of a number of regulatory units (RUs) and structural units (SUs). SUs define cellular behaviors, such as cell division, cell death or the production of transcription factors (TFs) for intra- and inter-cellular interactions. Whether the SUs of a gene are expressed is determined by the activity level of the RUs of the gene, refer to Fig. 2. Note that a single or multiple RUs may regulate the expression of a single or multiple SUs and that RUs can be activating ( $RU^+$ ) or repressive ( $RU^-$ ). The activation level of RUs is influenced by the TFs that can “bind” to the RU. If the difference between the affinity values of a TF and a RU is smaller than a predefined threshold  $\epsilon$  (in this work  $\epsilon$  is set to 0.2), the TF can bind to the RU to regulate the gene activation. The affinity values are encoded in the RUs and the SUs that produce a TF and are, as well as all values in the genome, limited to an interval of  $[0, 1]$ . The affinity similarity ( $\gamma_{i,j}$ ) between the  $i$ -th TF and  $j$ -th RU is defined by:

$$\gamma_{i,j} = \max(\epsilon - |\text{aff}_i^{\text{TF}} - \text{aff}_j^{\text{RU}}|, 0). \quad (3)$$

If  $\gamma_{i,j}$  is greater than zero, then the concentration  $c_i$  of the  $i$ -th TF is checked whether it is above a threshold  $\vartheta_j$  defined in the  $j$ -th RU:

$$b_{i,j} = \begin{cases} \max(c_i - \vartheta_j, 0) & \text{if } \gamma_{i,j} > 0 \\ 0 & \text{otherwise} \end{cases}. \quad (4)$$

Thus, the activation level contributed by the  $j$ -th RU (de-

noted by  $a_j, j = 1, \dots, N$ ) can be calculated as follows:

$$a_j = \sum_{i=1}^M b_{i,j}, \quad (5)$$

where  $M$  is the number of TFs that bind to the  $j$ -th RU. Assume the  $k$ -th gene is regulated by  $N$  RUs, the expression level of the gene can be defined by

$$\alpha = g(\mathbf{c}), \quad (6)$$

$$g_k(\mathbf{c}) = 100 \sum_{j=1}^N l_j a_j (2s_j - 1), \quad s_j \in (0, 1). \quad (7)$$

$2s_j - 1$  denotes the sign (positive for activating and negative for repressive) of the  $j$ -th RU and  $l_j$  is a parameter representing the strength of the  $j$ -th RU. If  $\alpha_k > 0$ , then the  $k$ -th gene is activated ( $\delta_k = 1$ ) and its corresponding behaviors coded in the SUs are performed.

An SU that produces a TF ( $SU^{\text{TF}}$ ) also encodes all parameters related to the TF, such as the affinity value, the decay rate  $D_i^c$ , the diffusion rate  $D_i^f$ , as well as the amount of the TF $_i$  to be produced. Which TF $_i$  is produced is defined in terms of the affinity value.

$$\mathbf{A} = \mathbf{h}(\boldsymbol{\alpha}), \quad h_i(\alpha_k) = \begin{cases} \beta \left( \frac{2}{1 + e^{-20 \cdot f \cdot \alpha_k}} - 1 \right) & \text{if } \alpha_k > 0 \\ 0 & \text{otherwise} \end{cases}, \quad (8)$$

where  $f$  and  $\beta$  are both encoded in the  $SU^{\text{TF}}$ .

A TF produced by an SU can be partly internal and partly external. To determine how much of a produced TF is external, a percentage ( $p^{\text{ext}} \in (0, 1)$ ) is also encoded in the corresponding gene. Thus,  $\Delta c_i^{\text{ext}} = p^{\text{ext}} \cdot A_i$  is the amount of external TF to be produced and  $\Delta c_i^{\text{int}} = (1 - p^{\text{ext}}) \cdot A_i$  is that of the internal TF.

External TFs are put on four grid points around the center of the cell, which undergo first a diffusion and then a decay process. Note, that the external TFs are computed on a grid but the positions of the cells are continuous and therefore not limited to this grid. The internal TFs underlie only a decay process. All internal and external concentrations of TFs are limited to an interval of  $[0, 1]$ .

Figure 3 shows a block diagram of the main components of a GRN in one cell, describing the cell dynamics. The cell dynamics can become coupled through external transcription factors, which underlie a diffusion and decay process and are position dependent. The number of TFs involved in gene regulation of the cellular behaviors is defined by the genome and the parameters in the resulting GRN as well. The number of cells also changes during development, starting with one single cell and two external TFs. The maximum number of cells is limited to 700 cells for reducing computational cost. From a control system point of view, the developmental system is composed of a changing number of

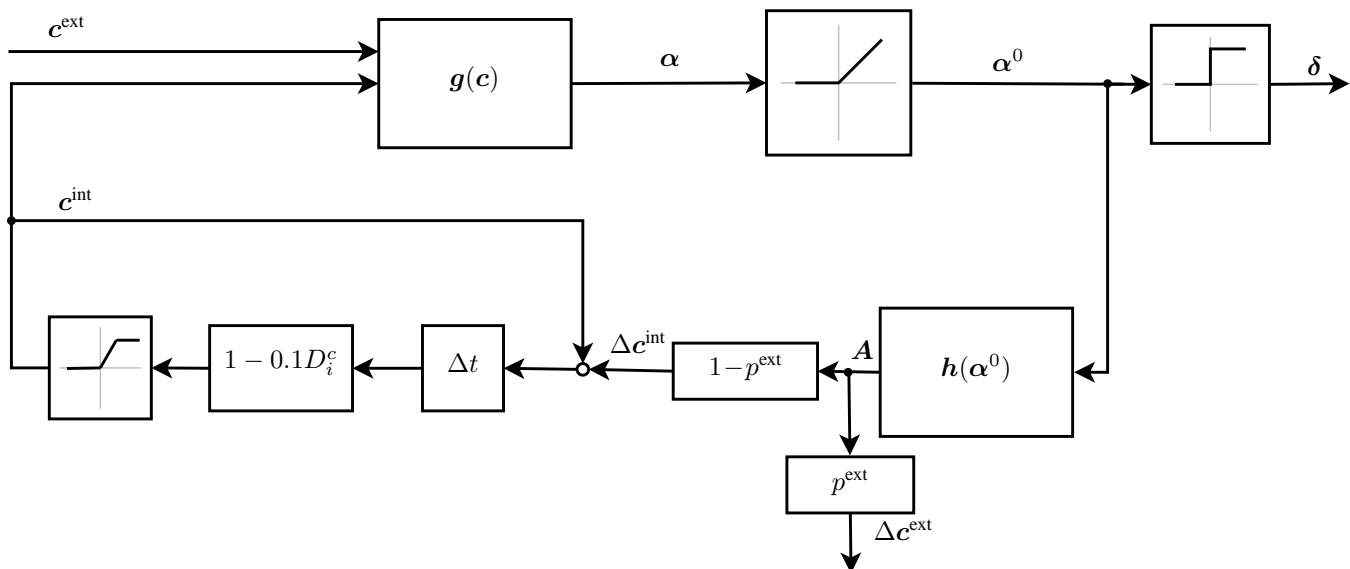


Figure 3: Block diagram of the model of a single cell.

nonlinear dynamical sub-systems with a changing number of system states, and the dynamics of the sub-systems are strongly coupled with each other.

In our experiments, we put two prediffused, external TFs without decay and diffusion in the computation area. The first TF has a constant gradient in the  $x$ -direction and the second in  $y$ -direction.

The SU for cell division ( $SU^{\text{div}}$ ) encodes the angle of division, indicating where the daughter cell is placed. A cell with an activated SU for cell death ( $SU^{\text{die}}$ ) dies at the developmental timestep it is activated. When both cell death and cell division are active at the same developmental step, only cell death is performed.

A cell with an active SU for neuron formation ( $SU^{\text{neuron}}$ ) becomes a CPG for the rest of its lifetime. All cells on the outside of the individual that are not CPGs at the end of the development are termed muscle cells. The threshold for whether the  $i$ -th CPG is to be connected to the  $j$ -th CPG is calculated as follows:

$$\varphi_{ij} = \frac{c_1}{1 + e^{c_2 \cdot (d_{ij} - 10c_3)}}, \quad (9)$$

where  $d_{ij}$  is the distance between the  $i$ -th and  $j$ -th neuron and  $c_1$ ,  $c_2$  and  $c_3$  are encoded in the  $SU^{\text{neuron}}$ . Then, a random number  $p$  ( $p \sim \mathcal{N}(0, 1)$ ) is generated, and if  $p < \varphi_{ij}$ , a connection between the two CPGs will be generated.

There is one additional SU for other possible actions, which are not used in this work. As a result, it can happen that some genes perform no action, that is one cause of redundancy.

The muscle cells contract with the output of one of the neurons of the closest CPG. When the distance to the closest CPG is higher than 8, the muscle cell is passive. A contrac-

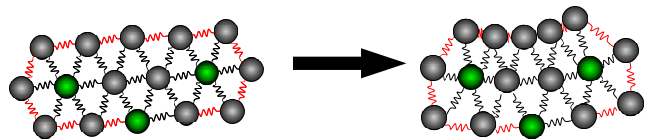


Figure 4: Illustration of a body plan consisting of cells connected by springs. The CPGs are depicted in green. The springs on the outside of the body (red) are able to change their natural length, except the springs associated to a CPG.

tion of a muscle cell means a change in the rest length of the associated spring at the outside of the individual (counter-clockwise).

Since each CPG contains two neurons ( $u$  and  $v$ ), an orientation of the CPG is introduced to define to which neuron a cell is connected. The orientation of the CPG itself is defined by the gradient of a TF, which TF is used is defined in the SU for neuron formation. Parameter  $s_4$  in the SU defines an affinity value, the TF with the closest affinity to the affinity encoded in  $s_4$  is used for the orientation of the CPG. Cells which connect to the CPG on its first  $0 - 180^\circ$  are connected to the neuron  $u$  and cells connected with an angle of  $180 - 360^\circ$  are connected to the neuron  $v$  of the CPG.

## Physics Simulation

The physics simulation engine used to simulate the behavior of the animats is BREVE<sup>2</sup>

A simple model for simulating the effects of water forces is added, which has also been adopted in (Sfakiotakis and Tsakiris, 2006). In this model, the water forces for different

<sup>2</sup>see [www.spiderland.org/](http://www.spiderland.org/)

Table 2: Constants for the mechanical simulation environment

Mass of cells $m$	0.5
Radius of cells $r$	0.5
Damping constant $d$	1
Spring strength $c$	5
Normal natural length of springs $l_n$	2
Short natural length of springs $l_s$	1.2
Minimal periodic time $T_{min}$	10
Maximal periodic time $T_{max}$	400
Simulation length $t_{sim}$	500.0

elements  $i$  (sphere of the  $i$ -th cell) are computed as follows:

$$\mathbf{F}^i = \mathbf{F}_T^i + \mathbf{F}_N^i, \quad (10)$$

$$\mathbf{F}_T^i = -\lambda_T \cdot \text{sgn}(\mathbf{v}_T^i) \cdot (\mathbf{v}_T^i)^2, \quad (11)$$

$$\mathbf{F}_N^i = -\lambda_N \cdot \text{sgn}(\mathbf{v}_N^i) \cdot (\mathbf{v}_N^i)^2, \quad (12)$$

where  $\lambda_T$  and  $\lambda_N$  are the drag coefficients for each direction.  $\lambda$  depends on the effective area, a shape coefficient of the element and the fluid density.  $\mathbf{v}_T^i$  and  $\mathbf{v}_N^i$  are the velocities of element  $i$  in normal and tangential direction.  $\lambda_T = 0.001$  and  $\lambda_N = 2.5$  are used in this work. The water forces are computed for cells in the outside of the body plan. The normal and tangential vectors of the body parts ( $i$ -th sphere) can be calculated by:

$$\mathbf{t}^i = \frac{\mathbf{p}^{i-1} - \mathbf{p}^{i+1}}{|\mathbf{p}^{i-1} - \mathbf{p}^{i+1}|}, \quad (13)$$

$$\mathbf{n}^i = \begin{pmatrix} 0 & -1 \\ 1 & 0 \end{pmatrix} \cdot \mathbf{t}^i, \quad (14)$$

where  $\mathbf{p}^i$  is the position vector of the  $i$ -th cell and  $\mathbf{p}^{i-1}$  and  $\mathbf{p}^{i+1}$  are the positions of the neighboring cells on the outside of the morphology.

$$\mathbf{v}_N^i = \mathbf{n}^i \cdot \mathbf{v}^i, \quad (15)$$

$$\mathbf{v}_T^i = \mathbf{t}^i \cdot \mathbf{v}^i, \quad (16)$$

where  $\mathbf{v}^i$  is the velocity of the  $i$ -th cell.

## Experiments

The goal of the experiments is to evolve individuals that swim the furthest in a desired time. The fitness function for swimming is defined as follows:

$$f_{swim} = - \left| \left( \sum_{i=0}^n \mathbf{x}^i(t=0) \right) - \left( \sum_{i=0}^n \mathbf{x}^i(t_{end}) \right) \right|, \quad (17)$$

so the center of mass of the individual at the beginning and the end of the swimming period are computed and the distance is calculated.

Table 3: Properties of the evolutionary optimization

$\mu$	45
$\lambda$	300
Elitists	3
initial # RUs and SUs	50, 50
$\sigma$	$10^{-4}$
$p_{dup}, p_{trans}, p_{del}$	0.05, 0.03, 0.02

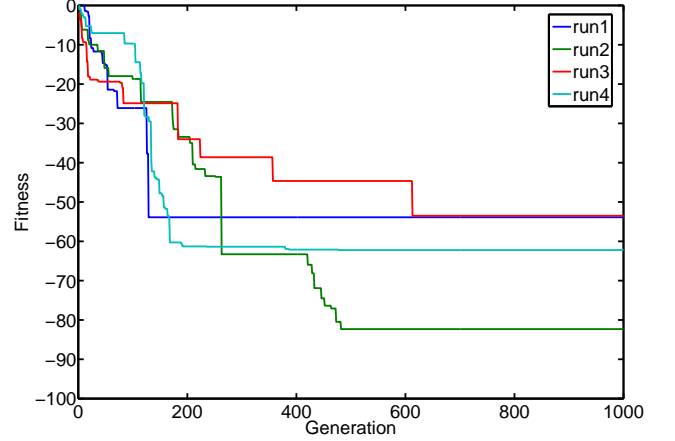


Figure 5: Fitness curves to evolve swimming individuals, their movements are controlled by CPGs.

The size of the individuals is limited, so the number of cells ( $n_c$ ) is constrained between 10 and 500. A penalty of  $600 - n_c$  will be applied if  $n_c < 10$  and a penalty of  $n_c$  if  $n_c > 500$ . If the cells in the developed morphology are not fully connected, a poor fitness of 100 will be assigned.

When the individual consists only of neurons or has no neurons, there will be no movement and the fitness for swimming is therefore set to zero ( $fit_{swim} = 0$ ). If the CPGs are not connected, which means there is no path to another CPG via synapses, the CPGs cannot synchronize and their phase shift is random and therefore depends on the initial values of the differential equation. To avoid that not connected CPGs get established during the evolution, but still not to penalize it too strong, the fitness for swimming is then halved.

The EA setup is defined in Table 3, four different runs with different random seeds have been performed.

## Results

The fitness curves of the four different runs are shown in Figure 5. The resulting individuals all swim between 53 and 82 length units (53.9, 82.3, 53.5, 62.2). Run 2 is analyzed in more detail in the following section.

### Analysis of Run 2

The fitness curve and the morphologies of some individuals from run 2 are shown in Figure 6. An elongated shape de-

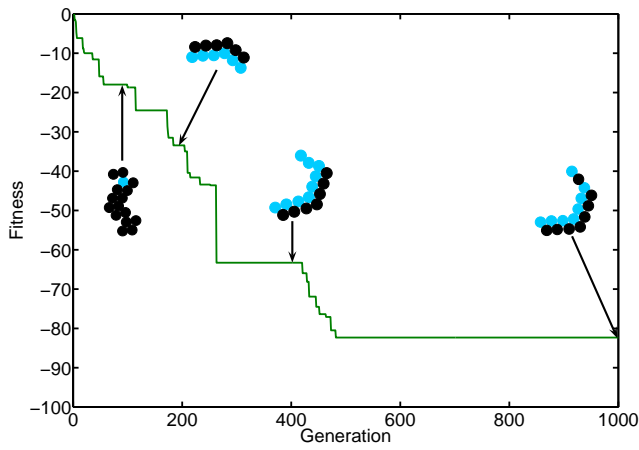


Figure 6: Fitness curve of run 2. The morphologies of the best individuals of generation 90, 200, 400 and 999 are drawn.

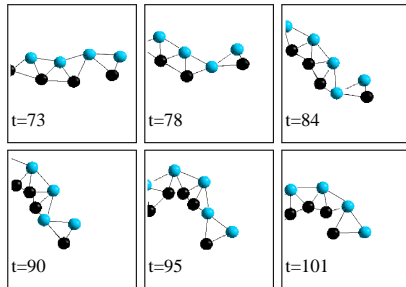
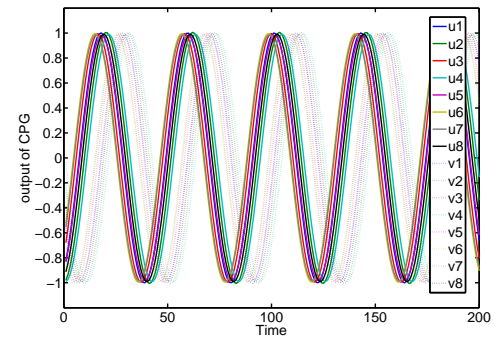


Figure 9: Tail fin of the best individual of run 2. Blue cells are CPGs, all other cells are black.

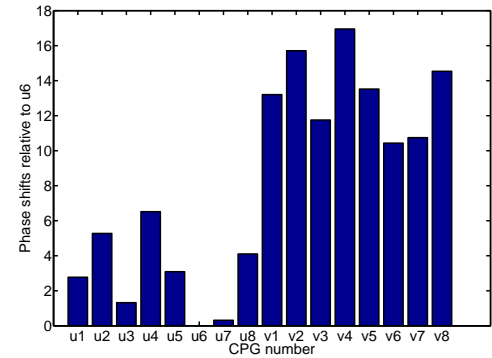
velops quickly (generation 90), and subsequently the shape smoothens in later generations. The number of the CPGs also increases and their positions change.

Figure 7 shows the development of the best individual of run 2, while Figure 8 shows its swimming behavior. Most cells first divide, transform to a CPG and die afterwards. Because of the neurons on one side of the individual, the springs on this side do not change their natural length and the movement of the individual is only caused by the springs on the other side of the individual. At the end of the individual a triangle forms which has the appearance and seems to fulfill the function of a tail fin, as shown in Figure 9. It is also interesting that the resulting individual is unsymmetric, contrary to the results of Jones et al. (2008) that show the advantage of symmetric morphologies.

The output of the CPGs are plotted in Figure 10, which shows that the phase shifts between the different CPGs are small. Figure 11 shows the orientations of the CPGs and we can see that some CPGs are turned around which results in a larger phase shift for the muscle cells.



(a) Time series of the different neurons.



(b) Phase shifts between the sinus curves of the different neurons relative to u6.

Figure 10: Output of all CPGs from the best individual of run 2.

## Summary and Outlook

In this paper, we have proposed a model that follows an animat's cell doctrine, i.e., an evolved gene regulatory network controls the cellular growth of a digital organism whose behavioral control is realized by some of the cells differentiating into central pattern generator cells representing neurons. Therefore, morphology and control of the animat are not merely co-evolved but co-represented by one regulatory system whose parameters are optimized during the evolutionary search process. Both on the genotypic and on the phenotypic level the distinction between morphology and control merely becomes descriptive.

The evolutionary optimization of the gene regulatory network resulted in a simple animat that is capable to perform swimming behavior by plausible movement. Body cells that differentiated into central pattern generators provide the ability to obtain an oscillating pattern with only a few neurons without limiting the connections or requiring long learning phases. In some cases the evolved morphology includes structures resembling tail fins, which seem to ease the functional or behavioral task. In principle, this is similar to the example of the passive walker that we mentioned in the introduction, where the dynamic control is eased by the



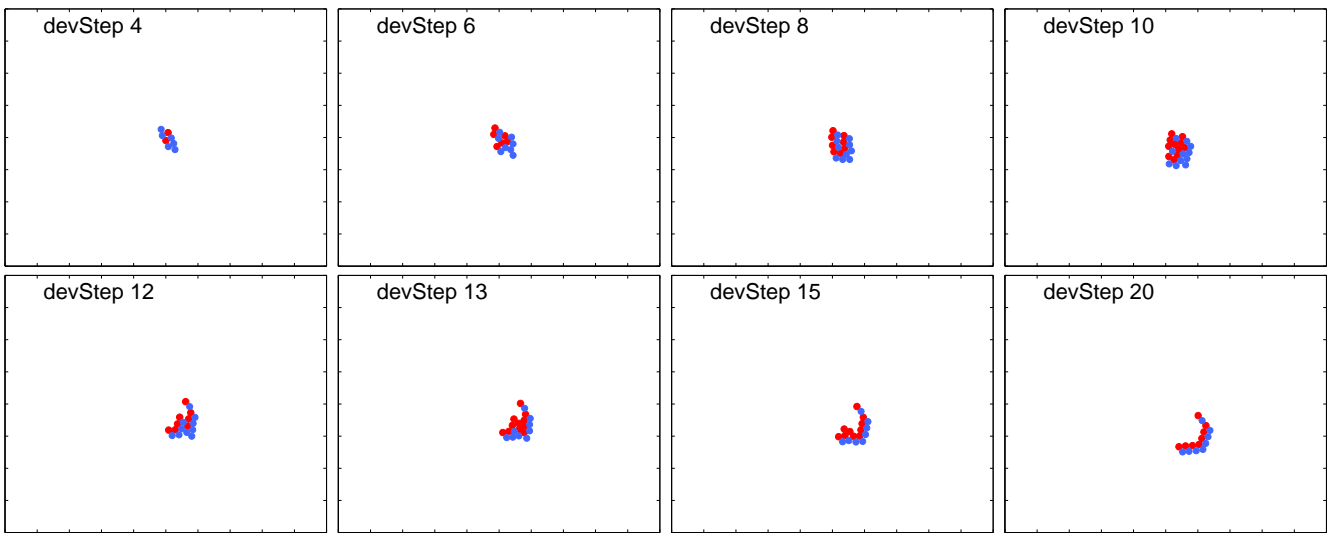


Figure 7: The development of the best individual of run 2 at the end of the evolution. Blue cells will divide in the next timestep, red cells transform to a CPG and will die in the next timestep.

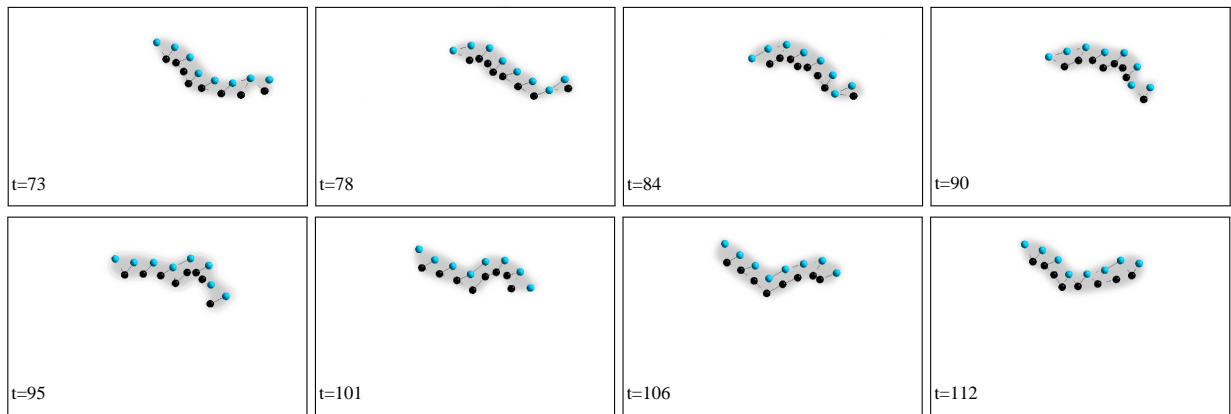


Figure 8: Swimming behavior of the best individual of run 2. Blue cells are CPGs, all other cells are black.

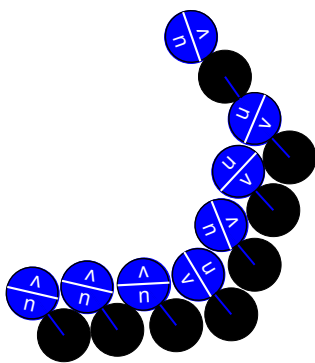


Figure 11: Orientation of the CPGs of the best individual of run 2. Since some CPGs are turned around, some muscle cells are connected to  $u$  and some to  $v$ , which causes the large phase shifts between the contractions of the springs.

morphology of the organism.

Compared to the work of Jones et al. (2011, 2008), which is based on a more abstract representation which is less biologically inspired, the evolved organisms do not exhibit symmetric morphologies. It would be interesting to find out under which constraints symmetry would also evolve in our framework.

The target of this research has been to demonstrate that the evolution of organisms exhibiting simple but meaningful behavior based on an animat's cell doctrine is possible. Finding the right parametrization of the gene regulatory network to develop a suitable morphology that incorporates the adjusted neural control is not a trivial task. At the same time, it is now necessary to analyze the properties of our model in more detail. First steps have been made in Figure 6 where we have observed the evolutionary path of the morphology for one run and in Figure 10 where we have analyzed how

the control is organized with the central pattern generator neurons. One of the next steps would be to relate the evolution of morphology to the evolution of the dynamics of the CPGs and how both are over time represented in the gene regulatory network. Unfortunately, even for digital evolution, the functional analysis of gene regulatory networks is a rather complex task, although promising first results have been obtained for evolving cellular morphologies, see e.g. Schramm et al. (2010).

## Acknowledgements

This work was supported by the Honda Research Institute Europe.

## References

- Andersen, T., Newman, R., and Otter, T. (2009). Shape homeostasis in virtual embryos. *Artificial Life*, 15(2):161–183.
- Beer, R. D. (2009). *Beyond Control: The Dynamics of Brain-Body-Environment Interaction in Motor Systems*, pages 7–24. Springer.
- Bongard, J. (2003). *Incremental Approaches to the Combined Evolution of a Robot's Body and Brain*. PhD thesis, University of Birmingham.
- Bongard, J. C. and Paul, C. (2000). Investigating morphological symmetry and locomotive efficiency using virtual embodied evolution. In *Proceedings of the SAB 2000*, pages 420–429.
- Chung, S.-J. and Slotine, J.-J. (2010). On synchronization of coupled hopf-kuramoto oscillators with phase delays. *arXiv:1004.5366v1*.
- de Jong, H. (2002). Modeling and simulation of genetic regulatory systems: A literature review. *Journal of Computational Biology*, 9(1):67–103.
- Doursat, R. (2009). Facilitating evolutionary innovation by developmental modularity and variability. In *Proc. of the GECCO 09*, pages 683–690.
- Eggenberger Hotz, P., Gómez, G., and Pfeifer, R. (2003). Evolving the morphology of a neural network for controlling a foveating retina - and its test on a real robot. In *Proc. of the ALife VIII*, pages 243–251.
- Harding, S. and Banzhaf, W. (2008). Artificial development. In Würz, R. W., editor, *Organic Computing*, chapter 9, pages 201–219. Springer.
- Hornby, G. and Pollack, J. (2001). Evolving L-systems to generate virtual creatures. *Computers & Graphics*, 25:1040–1048.
- Ijspeert, A. J. and Kodjacobian, J. (1999). Evolution and development of a central pattern generator for the swimming of a lamprey. *Artificial Life*, 5(3):247–269.
- Jin, Y., Schramm, L., and Sendhoff, B. (2008). A gene regulatory model for the development of primitive nervous systems. In *Proc. of the ICONIP 2008*, pages 48–55.
- Joachimczak, M. and Wròbel, B. (2009). Evolution of the morphology and patterning of artificial embryos: scaling the tricolour problem to the third dimension. In *Proc. of the ECAL 2009*.
- Jones, B., Jin, Y., Sendhoff, B., and Yao, X. (2008). Evolving functional symmetry in a three dimensional model of an elongated organism. In *Proc. of the ALife X*, pages 305–312.
- Jones, B., Soltoggio, A., Yao, X., and Sendhoff, B. (2011). Evolution of neural symmetry and its coupled alignment to body plan morphology. In *Proc. of the GECCO 2011*.
- Kitano, H. (1995). A simple model of neurogenesis and cell differentiation based on evolutionary large-scale chaos. *Artificial Life*, 2(1):79–99.
- Kowaliw, T., Grogono, P., and Kharma, N. (2004). Bluenome: A novel developmental model of artificial morphogenesis. In *Proceedings of GECCO 04*, pages 93–104.
- Mazzapioda, M., Cangelosi, A., and Nolfi, S. (2009). Co-evolving morphology and control: A distributed approach. In *Proc. of the CEC 2009*, pages 2217–2224.
- McGeer, T. (1990). Passive dynamic walking. *International Journal of Robotics Research*, 9(2):62–82.
- Meng, Y., Zhang, Y., Sampath, A., Jin, Y., and Sendhoff, B. (2011). Cross-ball: A new morphogenetic self-reconfigurable modular robot. In *Proc of the ICRA 2011*.
- Miconi, T. and Channon, A. (2006). An improved system for artificial creatures evolution. In *Proceedings of Artificial Life X*, pages 255–261.
- Murata, S. and Kurokawa, H. (2007). Self-reconfigurable robots. *Robotics & Automation Magazine, IEEE*, 14:71–78.
- Murray, J. D. (2008). *Mathematical Biology I: An Introduction*. Springer, third edition.
- Oros, N., Steuber, V., Davey, N., Cañamero, L., and Adams, R. (2009). Evolution of bilateral symmetry in agents controlled by spiking neural networks. In *IEEE Symposium on Artificial Life*, pages 116–123.
- Pfeifer, R., Lungarella, M., and Iida, F. (2007). Self-organization, and biologically inspired robotics. *Science*, 318(5853):1088–1093.
- Schramm, L., Jin, Y., and Sendhoff, B. (2009). Emerged coupling of motor control and morphological development in evolution of multi-cellular animats. In *Proc. of the ECAL 2009*.
- Schramm, L., Martins, V. V., Jin, Y., and Sendhoff, B. (2010). Analysis of gene regulatory network motifs in evolutionary development of multicellular organisms. In *Proc. of the ALife XII*, pages 133–140.
- Sfakiotakis, M. and Tsakiris, D. P. (2006). Simuun: A simulation environment for undulatory locomotion. *International Journal of Modelling and Simulation*, 26(4):350–358.
- Sims, K. (1994). Evolving virtual creatures. In *Proceedings SIGGRAPH*, pages 15–22.
- Spector, L., Klein, J., and Feinstein, M. (2007). Division blocks and the open-ended evolution of development, form, and behavior. In *Proceedings of GECCO*, pages 316–323.
- Stanley, K. O. and Miikkulainen, R. (2003). A taxonomy for artificial embryogeny. *Artificial Life*, 9(2):93–130.
- Steiner, T., Jin, Y., and Sendhoff, B. (2008). A cellular model for the evolutionary development of lightweight material with an inner structure. In *Proc. of the GECCO'08*, pages 851–858.
- Steiner, T., Trommler, J., Brenn, M., Jin, Y., and Sendhoff, B. (2009). Global shape with morphogen gradients and motile polarized cells. In *Proceedings of the 2009 Congress on Evolutionary Computation*, pages 2225–2232.
- Verdaasdonk, B. W., Koopman, B. F. J. M., and Helm, F. C. V. D. (2006). Energy efficient and robust rhythmic limb movement by central pattern generators. *Neural Networks*, 19(4):388–400.